Effects of Hydrophobic Surfactant Proteins on Collapse of Pulmonary Surfactant Monolayers

Florence Lhert, Wenfei Yan, Samares C. Biswas, and Stephen B. Hall
Departments of Biochemistry and Molecular Biology, Medicine, and Physiology and Pharmacology, Oregon Health & Science University, Portland, Oregon 97239

ABSTRACT To determine if hydrophobic surfactant proteins affect the stability of pulmonary surfactant monolayers at an air/water interface, the studies reported here compared the kinetics of collapse for the complete set of lipids in calf surfactant with and without the proteins. Monomolecular films spread at the surface of captive bubbles were compressed at 37°C to surface pressures above 46 mN/m, at which collapse first occurred. The rate of area-compression required to maintain a constant surface pressure was measured to directly determine the rate of collapse. For films with and without the proteins, higher surface pressures initially produced faster collapse, but the rates then reached a maximum and decreased to values <0.04 min^{-1} above 53 mN/m. The maximum rate for the lipids with the proteins (1.22 ± 0.28 min^{-1}) was almost twice the value for the lipids alone (0.71 ± 0.15 min^{-1}). Because small increments in surface pressure produced large shifts in the rate close to the fastest collapse, compressions at a series of constant speeds also established the threshold rate required to achieve high surface pressure as an indirect indication of the fastest collapse. Both samples produced a sharply defined threshold that occurred at slightly faster compression with the proteins present, supporting the conclusion of the direct measurements that the proteins produce a faster maximum rate of collapse. Our results indicate that at 47–53 mN/m, the hydrophobic surfactant proteins destabilize the compressed monolayers and tend to limit access to the higher surface pressures at which the lipid films become metastable.

INTRODUCTION

Pulmonary surfactant reduces surface tension in the lungs to impressively low values. When secreted by the type II pneumocytes into the thin liquid layer that lines the alveolar air spaces, vesicles of pulmonary surfactant adsorb rapidly to the air/water interface and form an interfacial film. Analyses by several approaches establish that when compressed by the decreasing alveolar surface area during exhalation, the adsorbed films reach very low surface tensions and sustain those values for prolonged durations in static lungs after compression stops (1–5). In contrast, under equilibrium conditions in vitro, interfacial monolayers undergo a phase transition that limits access to the high surface pressures (π) corresponding to these low surface tensions. Two-dimensional films collapse from the interface to form a three-dimensional bulk phase at the equilibrium spreading pressure (π_e) (6), which occurs for the phospholipids at $\leq$46 mN/m (7,8). In the lungs, π reaches values above 65 mN/m, indicating that the films avoid this transition and that they must be metastable.

Efforts to explain that metastability originally focused on the unusual composition, relative to other biological mixtures, of the surfactant phospholipids (9,10). More recent studies have suggested that the hydrophobic surfactant proteins, SP-B and SP-C, might also help stabilize the films. Although these proteins constitute only ~1–2% (w:w) of pulmonary surfactant, they represent the only constituents proven to be essential for its function. In genetically modified animals and babies with congenital abnormalities, breathing in the absence of SP-B injures the alveolocapillary barrier, leading to pulmonary edema and respiratory failure (11–13). Mice deficient in SP-C also develop pulmonary problems, although of a lesser degree and at a later age (14). Investigators have reported both that the proteins in bilayers produce an ordering of lipids (15–17), which in monolayers could result in more stable films, and that the proteins enhance the ability of monolayers to reach high π (18–23). These results suggest that in addition to their well-established ability to promote interfacial adsorption of the lipids (24–30), the proteins might also limit collapse of the compressed monolayer.

The studies, however, that suggest a stabilizing effect of the proteins have used model surfactants and experimental conditions with important deviations from physiological systems. The experiments here compared the kinetics of collapse at 37°C for the complete set of lipids in calf surfactant with and without the hydrophobic proteins. The results should reflect the full complexity of the biological mixture under more physiological conditions.

MATERIALS AND METHODS

Materials

Extracted calf surfactant (calf lung surfactant extract, CLSE), prepared as described previously (31), was obtained from ONY (Amherst, NY) and used without further purification. The complete mixture of neutral and phospholipids (N&PL) was obtained from CLSE by using gel permeation

Submitted May 10, 2007, and accepted for publication July 13, 2007.

Address reprint requests to Stephen B. Hall, Mail Code UHN-67, Oregon Health & Science University, Portland, OR 97239-3098. Tel.: 503-494-6667; E-mail: sbh@ohsu.edu.

Editor: Thomas J. McIntosh.

0006-3495/07/12/4237/07 $2.00

doi: 10.1529/biophysj.107.111823

chromatography to reduce the hydrophobic proteins from ~1.5% (w:w, assuming an average molecular mass for the phospholipids of 750 g/mol) to undetectable levels (32,33). Prior analysis has shown that this approach has no effect on the composition of headgroups, acyl groups, or cholesterol (17,32). Thin-layer chromatography (34) and biochemical assays (35,36) confirmed that the CLSE and N&PL used here contained the same composition of headgroups and cholesterol.

The following reagents were purchased commercially and used without further purification: high-purity chloroform and methanol (Burdick and Jackson, Muskegon, MI); NaCl (Mallinckrodt Specialty Chemical, Paris, KY); HEPES (Sigma, St. Louis, MO); and $CaCl_2 \cdot 2H_2O$ (J. T. Baker, Phillipsburg, NJ). Water was distilled and then passed through a multicartridge purification system (Macropure, Ultrapure DI and Organic-Free cartridges, Barnstead/Thermolyne, Dubuque, IA). All glassware was acid cleaned.

Methods

Biochemical assays

Phospholipid concentrations were determined by measuring the phosphate content of measured aliquots (35). Protein assays used the amido black method with bovine serum albumin as the standard (37). Cholesterol, including free and esterified compounds, was measured by reduction with ferrous sulfate (36).

Measurements with films

The ''surface balance'' used to determine the variation of π in response to changes in area consisted of a captive bubble floating below an agarose dome (38–41). Infusion and withdrawal of buffer by a computer-controlled syringe pump alters the volume of the bubble and regulates area. Because surface area depends on the shape of the bubble as well as its volume, control of area is indirect. Previous comparison of films on Langmuir troughs and captive bubbles have produced π–A isotherms on the two instruments that are equivalent (40). Measurements of the bubble's height and diameter provide π and area of the monolayer via a semiempirical algorithm (42,43). Relative to Langmuir troughs, captive bubbles allow easier regulation of temperature above ambient levels and compression at faster rates, including at the physiological rates that occur in the alveoli. The greatest advantage for these studies, however, is that confinement by the continuous interface of the bubble avoids any escape of the film along or around artificial barriers (44), which can confound measurements of collapse on Langmuir troughs.

To ensure that monolayers contained a defined set of constituents, samples were spread directly at the air/water interface of the bubble. The spreading solvent (chloroform:methanol, 1:1, v/v) was removed by circulating large volumes of buffer through the subphase (40). In the experiments reported here, samples of 0.08–0.09 μl at ~4 mM phospholipid were spread at the surface of a 90–130 μl bubble in buffered electrolyte (10 mM HEPES pH 7.0, 150 mM NaCl, 1.5 mM $CaCl_2$). The bubbles were maintained at 37°C using heating pads (Minco, Minneapolis, MN) applied along the sides of the chamber, with temperature monitored by a thermistor probe (YSI, Yellow Spring, OH) and manipulated by a controller (Cole-Palmer, Vernon Hills, IL).

Two kinds of experiments characterized the kinetics of collapse. First, isobaric measurements determined the change in area required to maintain constant π. An initial rapid infusion of buffer increased π above 45 mN/m. Frame-by-frame analysis of the bubble's profile provided the final π at the end of the pulsed compression. A computer program written in LabVIEW (National Instruments, Austin, TX) then manipulated the syringe pump using simple feedback to maintain that final π.

The second set of experiments instead determined the rate of compression required to reach high π. After slow compression to $\pi \approx 45$ mN/m, buffer was infused at different constant rates during a >47% change of the bubble's volume. Area decreased as an approximately linear function of time. Because the relation between volume and area depends on the shape of the bubble, different rates of compression through the same change in volume produced different changes in area. These differences in final area could theoretically affect the final π, with higher final π simply reflecting greater compression. Films that experienced the largest change in area (>58%), however, produced the lowest final π ($\leq$52.4 mN/m). Changes in area between 30% and 46% achieved final π between 54 and 69 mN/m.

RESULTS

Basic isotherms

During slow compression, N&PL exhibited isotherms similar to those obtained previously with CLSE (45), consisting of an initial continuous increase in π to ~46 mN/m, followed by a plateau, during which further compression produced much smaller increases in π (Fig. 1). Prior microscopic studies have shown that the plateau coincides with collapse of the compressed monolayer to form three-dimensional structures (46,47). More rapid compression of N&PL to higher π produced the same transformation demonstrated previously for CLSE, dimyristoyl phosphatidylcholine (DMPC), and 1-palmitoyl-2-oleoyl phosphatidylcholine (POPC) (41,45,48). The films showed minimal evidence of collapse not only after first achieving high π but also during slow expansion to $\pi < \pi_e$, followed by slow recompression (Fig. 1). Once the films reached high π, their resistance to collapse persisted after expansion to the initial conditions, at which they originally collapsed rapidly. Transformed films of N&PL, like DMPC and POPC, replicated the metastability of pulmonary surfactant in situ despite the absence of the surfactant proteins.

Directly measured rates of collapse

To determine how the hydrophobic proteins affect the stability of surfactant films, we compared the collapse of monolayers containing CLSE or N&PL (Figs. 2 and 3). These experiments assumed that under isobaric (constant π) conditions, molecular area is constant. For an isobaric collapsing film, the rate, $\dot{n}$, at which constituents leave the interface would then be directly related to the rate, $\dot{A}$, at which area changes (49), and the fractional rates, $\dot{n}/n$ and $\dot{A}/A$, at which interfacial constituents and area change, would be equal. Experiments here compressed the area of films slowly at 37°C to 45 mN/m, below π_e, and then rapidly ($\dot{A}/A \approx 32\ \text{min}^{-1}$) to higher predetermined levels of π. The rate of change in area necessary to maintain π constant at those higher values provided the rate of collapse.

In most cases with both CLSE and N&PL, experiments subjected the films to a slight overcompression (<3 mN/m, Figs. 2 and 3, *top traces*, *right axes*) before π stabilized at the desired value. For both samples, at each π investigated, surface area then decreased at slowing rates. The variation of area fit well to a simple exponential function of time (Figs. 2 and 3, *solid lines* at long times, *left axis*), as expected for a monomolecular film undergoing a first-order transition to a collapsed phase through an area of fixed dimensions (50).

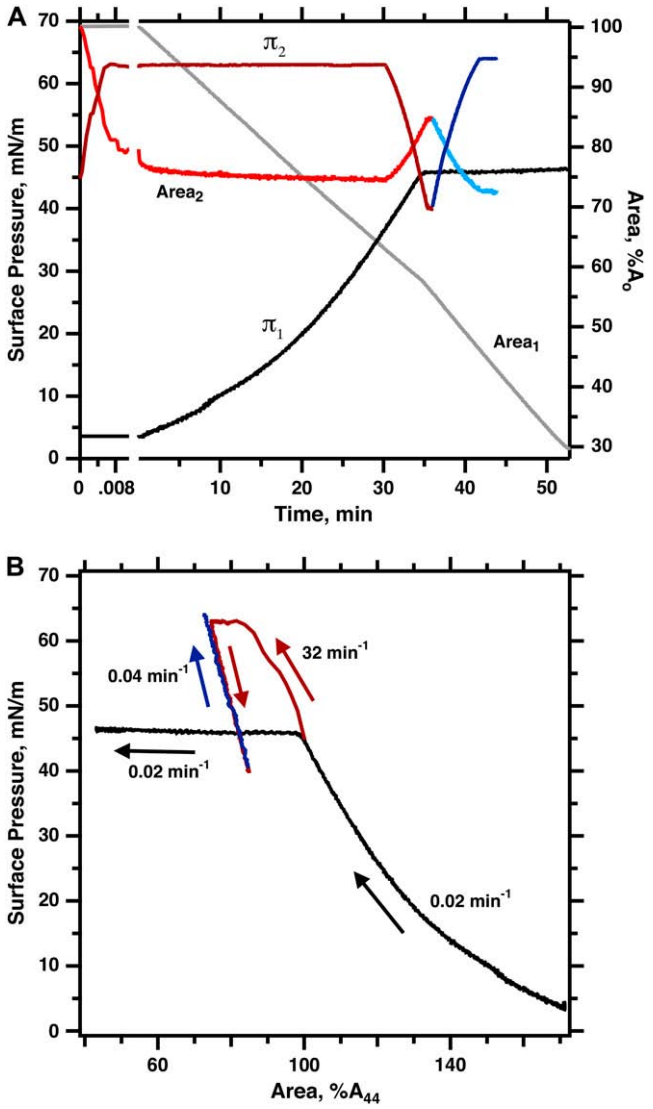

FIGURE 1 Variation of π and area during isothermal fast and slow compressions for N&PL. Films were spread on the surface of a captive bubble, heated to 37°C, and compressed either continuously at 0.02 min^{-1} (experiment 1, *black/gray lines*), or during a brief pulse at 32 min^{-1}, after which area was expanded and recompressed at 0.04 min^{-1} (experiment 2, *red/blue lines*). Rates of compression are expressed as $A^{-1}\cdot dA/dt$. (*A*) π (*left axis*) and area (*right axis*) versus time after beginning of compression. The subscripts indicate data from the same experiment. Surface area is expressed relative to the initial value (A_o) at the beginning of compression from different initial π values. (*B*) The same data expressed as π-area isotherms. Surface area is expressed relative to the value at 44 mN/m (A_{44}) during the initial compression to facilitate comparison of different experiments. Arrows indicate the temporal progression of the measurements.

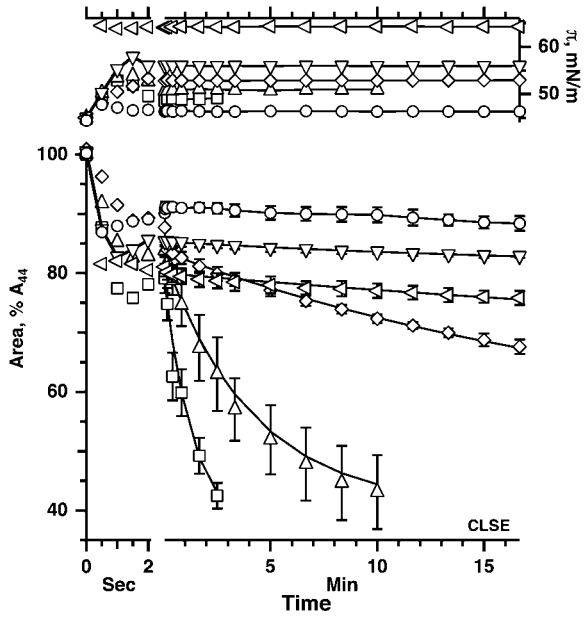

FIGURE 2 Kinetics of isobaric collapse for spread films of CLSE. Data indicate the temporal variation of π (*shaded symbols*, *right axis*) and area (*solid symbols*, *left axis*) during an initial rapid change in area (initial portion of split time axis) followed by an isobaric compression (later time). Each symbol represents the mean of measurements at selected times for at least three experiments, ± standard deviation for area during the isobaric compression. Data at additional times and other π-values were omitted for purposes of clarity. Solid lines at times beyond 2 s give the best fit for data averaged at all times to the equation $[A(t) - A_\infty]/[A_o - A_\infty] = \exp(-kt)$, where $A(t)$, A_o, and A_∞ represent the surface area at times t, t_o = time at onset of constant π, and $t = \infty$ by extrapolation, respectively. Area is expressed relative to the value at 44 mN/m (A_{44}) before the pulsed compression.

Although molecular rearrangements within the monolayer could also cause surface area to decrease after pulsed compressions, previous studies at $\pi < \pi_e$, where collapse does not occur, indicate that such relaxations contribute <2% to the change in area (41). Relaxation was therefore ignored above π_e, and the time constant for the best fits to an exponential function was used to express the kinetics of collapse quantitatively.

At different π above π_e, the rate of collapse for both samples first increased with π, as expected with further deviation above π_e, but then reached a maximum (Fig. 4). The rate of collapse then decreased at higher π and, above 56 mN/m, reached values that were <2% of the maximum. The same behavior has been observed previously for monolayers of pure POPC (41). Once the films reached π of 53 mN/m or higher, CLSE and N&PL, like POPC (51), were stable for hours (data not shown).

The presence of the hydrophobic proteins shifted the π of the fastest collapse to slightly higher values, from ~46.7 mN/m for N&PL to ~48 mN/m for CLSE (Fig. 4). The maximum rate of collapse for the complete mixture with the proteins (1.20 ± 0.24 min^{-1} for CLSE) was almost twice the highest rate (0.72 ± 0.12 min^{-1} for N&PL) for the same lipids without the proteins. Collapse remained faster for CLSE over the range of π from 47 to 51 mN/m. Above 51 mN/m, rates of collapse for CLSE and N&PL became approximately equal. The hydrophobic proteins SP-B and SP-C favored collapse just above π_e, but at higher π, films with or without the proteins both became metastable.

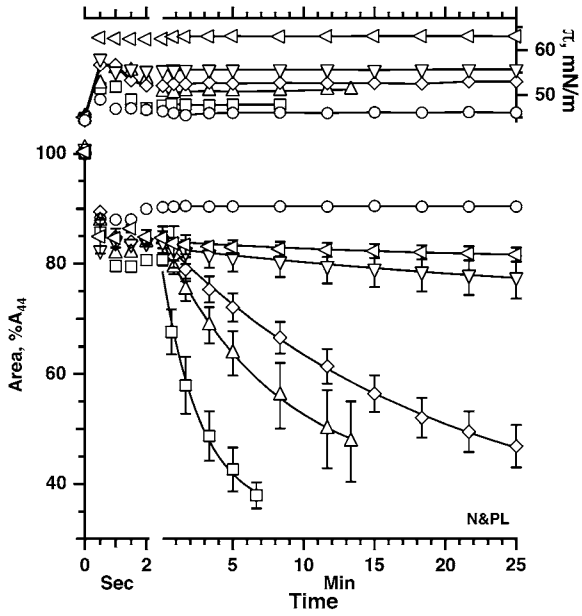

FIGURE 3 Kinetics of isobaric collapse for spread films of N&PL. Conditions are the same as in Fig. 2.

Threshold rates of compression

Small changes in π produced large changes in the rates of collapse close to the maximum values (Fig. 4). This characteristic raised concern that determination of the true maximum rate might be difficult, and specifically that our measurements of collapse at limited values of π might have missed the fastest rates. A second set of experiments therefore used a different approach to establish how the proteins affected collapse. Rather than using isobaric compressions at different π, experiments instead compressed bubbles at a series of constant rates. During compression, π increases only as long as compression is faster than collapse (52). When the two processes occur at equal rates, π remains unchanged. Because the rate of collapse rises steeply to a maximum value at a π close to π_e, progressively faster compression should produce little change in π as long as the rate remains slower than the fastest collapse. Any compression, however, which exceeds that maximum rate should reach the same final high π. Compression at progressively faster rates should therefore exhibit a threshold, with the final π initially rising minimally above π_e, but then abruptly increasing to high values >65 mN/m. This threshold rate of compression for achieving high π provides a qualitative index of the fastest collapse and an alternative method for establishing how the proteins affect collapse.

Films of N&PL and CLSE compressed at different rates both showed the threshold predicted by the directly measured rates of collapse. Very slow compression increased π from π_e of 46 to a final value of ~50 mN/m (Figs. 5 and 6). Further increases in rate initially produced little change (Fig. 5 for N&PL; data not shown for CLSE). For both films, the final π increased abruptly to values above 65 mN/m over a remarkably narrow range of compression speeds (Fig. 6). The experiments confirmed our original observation of a threshold rate for CLSE (45), obtained with a different pattern of compression, and extended the findings to N&PL.

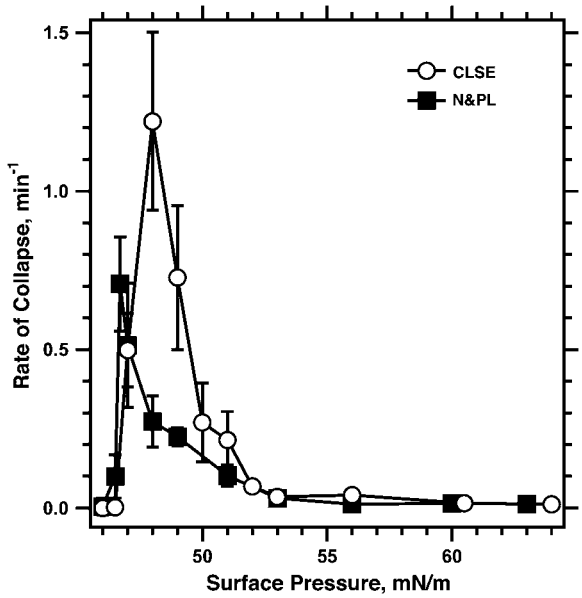

FIGURE 4 Effect of hydrophobic surfactant proteins on the kinetics of collapse. Symbols represent the rate of collapse (mean ± SD) obtained from the time constant k, defined in the legend for Fig. 2, for the experimental curves fit to the area during isobaric compression at different π-values. $n \geq 3$ for each set of measurements.

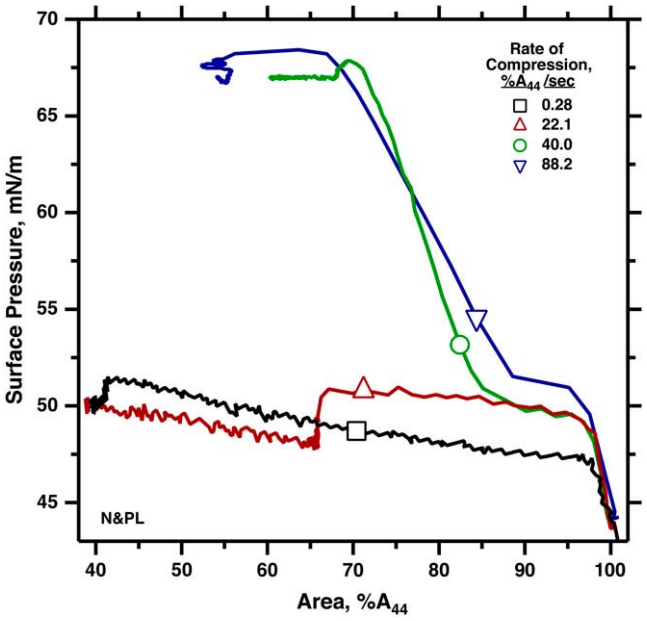

FIGURE 5 Variation of π during compression of N&PL monolayers at different approximately constant rates. Buffer infused at different constant rates produced roughly linear changes in area with time. Area is expressed relative to the initial value (A_{44}) at 44 mN/m.

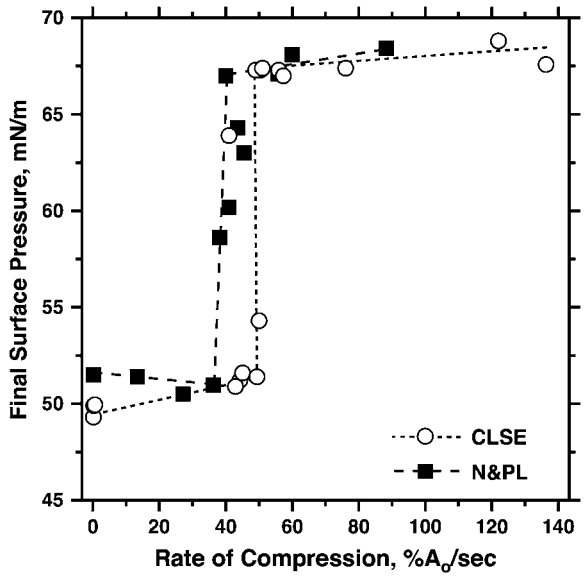

FIGURE 6 Effect of surfactant proteins on the final π achieved during compression at different constant rates for CLSE and N&PL. Experiments were conducted as illustrated in Fig. 5. Dashed lines connect the points for the highest rate with a final $\pi < 52$ mN/m and the lowest rate with $\pi > 65$ mN/m, for purposes of illustration only.

The threshold rates for CLSE and N&PL were similar (Fig. 6). The jump in the final π from ~52 to ~67 mN/m occurred over a range of rates that was slightly lower for N&PL than for CLSE, consistent with the faster collapse for CLSE suggested by the directly measured rates (Fig. 4). The similar threshold rates argue that the destabilizing effects of the proteins may be smaller than suggested by the directly measured rates of collapse. They also indicate that the surfactant monolayer is not stabilized by the hydrophobic proteins.

DISCUSSION

The results reported here show that the hydrophobic surfactant proteins are unnecessary to stabilize surfactant monolayers at high π. If they reach $\pi \geq 55$ mN/m, monomolecular films of the surfactant lipids become metastable, with rates of collapse that are low, with or without the proteins. Rather than having a stabilizing effect, as suggested by several prior studies (18–23), the proteins at the lower π between 47 and 51 mN/m actually increase rates of collapse. The two methods used to characterize the kinetics of collapse suggest different extents of destabilization. The directly measured highest rate of collapse with the proteins present is almost twice the value for the lipids alone. The threshold rate of compression required to reach high π, which provides an indication of the fastest collapse that is indirect but possibly more accurate, argues that the destabilizing effect is more limited. With both approaches, however, the results are inconsistent with a major increase in the resistance to collapse caused by the proteins.

Physiological data provide no contradiction of these findings. The consequences of their absence indicate that the proteins provide a necessary function (11–13,53,54), but their well-known ability to promote interfacial insertion (23, 24,26–30,55) adequately explains their essential role. Measurements concerning the alveolar films indicate only their metastability. Films containing lipids, whether in the tilted-condensed (40,44) or supercompressed-fluid state (41,45,51), replicate that metastability without the proteins. The available physiological data and the studies here provide no evidence for a second activity of the protein in stabilizing the interfacial monolayer.

Our results agree with several structural studies that show that the proteins can facilitate collapse of surfactant films (56–59). The proteins apparently promote movement of the lipids both into and from the air/water interface. They are well known to accelerate insertion of the phospholipids into an expanding interface, whether by adsorption of surfactant vesicles (24,25,27–30) or respreading of collapsed material (20,22,55–58,60). Their effect on collapse may simply reflect promotion of the reverse process. The proteins would then act as catalysts, reducing the energy barrier between the interfacial monolayer and adjacent bilayers, and accelerating conversion between the two states in both directions.

Several investigators have suggested that the effects of the proteins on collapse might be beneficial. The proteins promote collapse into structures that readily respread (23,55,57,58,61), and the pool of collapsed constituents can help sustain a saturated film on an expanding interface. The physiological importance of respreading, however, is difficult to confirm. The extent to which the alveolar film collapses is unknown, and no circumstances exist under which insertion of material into an expanding interface could not instead occur by adsorption of new vesicles. The well-established dependence in vitro of pulsating bubble experiments on concentration in the subphase (62), which should affect adsorption but not respreading, suggests that when both processes are possible, adsorption may dominate. In contrast to respreading, the physiological relevance of slow collapse is well established by the persistently high π in static lungs (1,3). The important physiological question is not how the proteins produce collapse to structures that respread, but rather how the alveolar films avoid collapse of any form.

The opposite conclusions reached here and previously concerning how the proteins affect the stability of the surfactant film presumably reflect differences in experimental design and chemical composition. Measurements that include surfactant in the subphase, such as with Enhorning's pulsing bubble apparatus or with surfactant-deficient lungs, complicate efforts to distinguish between effects of the proteins on interfacial insertion and stability of the film (18). The composition of model systems used in previous studies has also differed from the physiological mixtures in important ways (18–23). These include a focus on palmitic acid, which native surfactant contains in minimal amounts, and the omission of

cholesterol, which in phospholipid systems converts coexisting solid and fluid phases to two fluid phases (33,63). Model systems provide simplified systems that can facilitate the testing of hypotheses concerning the mechanisms by which physiological processes occur. To define the basic phenomena that should be modeled, however, physiological mixtures seem more appropriate.

Our studies are subject to the reservation that they considered only monomolecular films. The experiments leave open the possibility that the proteins might stabilize a multilayer. Microscopic studies have shown that at least portions of the alveolar film contain multiple layers (64,65). In addition to the extensive evidence that multilayers can form by collapse, recent studies demonstrate that they can also form by adsorption (66). A multilayer would then exist during the first exhalation, when the surfactant film apparently is already fully functional. The extent to which additional adsorbed layers would stabilize a monolayer is uncertain. The multiple layers formed by collapse apparently do not impede further collapse, which frequently occurs from multilamellar rather than monomolecular regions of the film (47,56,58). Collapsed multilayers, however, may form via discrete structures that connect the different layers (47) and that might be absent from an adsorbed multilayer. Whether the proteins affect formation of an adsorbed multilayer, and whether the additional layers with or without the proteins affect the kinetics of collapse remain unknown.

SUMMARY

The results reported here show that monomolecular films containing only the surfactant lipids without the proteins achieve and sustain the high π observed in the lungs. The hydrophobic surfactant proteins, rather than stabilizing the lipid films, instead increase the rates of collapse.

CLSE was a gift from Dr. Edmund Egan, Ony, Amherst, NY. These studies were funded by the National Institutes of Health (HL60914).

REFERENCES

1. Horie, T., and J. Hildebrandt. 1971. Dynamic compliance, limit cycles, and static equilibria of excised cat lung. *J. Appl. Physiol.* 31:423–430.
2. Wilson, T. A. 1981. Relations among recoil pressure, surface area, and surface tension in the lung. *J. Appl. Physiol.* 50:921–930.
3. Schürch, S. 1982. Surface tension at low lung volumes: dependence on time and alveolar size. *Respir. Physiol.* 48:339–355.
4. Valberg, P. A., and J. D. Brain. 1977. Lung surface tension and air space dimensions from multiple pressure-volume curves. *J. Appl. Physiol.* 43:730–738.
5. Smith, J. C., and D. Stamenovic. 1986. Surface forces in lungs. I. Alveolar surface tension-lung volume relationships. *J. Appl. Physiol.* 60:1341–1350.
6. Gaines, G. L. 1966. Insoluble Monolayers at Liquid-Gas Interfaces. Interscience Publishers, New York.
7. Phillips, M. C., and H. Hauser. 1974. Spreading of solid glycerides and phospholipids at the air-water interface. *J. Colloid Interface Sci.* 49: 31–39.
8. Lee, S., D. H. Kim, and D. Needham. 2001. Equilibrium and dynamic interfacial tension measurements at microscopic interfaces using a micropipet technique. 1. A new method for determination of interfacial tension. *Langmuir.* 17:5537–5543.
9. Clements, J. A. 1977. Functions of the alveolar lining. *Am. Rev. Respir. Dis.* 115:67–71.
10. Bangham, A. D., C. J. Morley, and M. C. Phillips. 1979. The physical properties of an effective lung surfactant. *Biochim. Biophys. Acta.* 573: 552–556.
11. Nogee, L. M., G. Garnier, H. C. Dietz, L. Singer, A. M. Murphy, D. E. deMello, and H. R. Colten. 1994. A mutation in the surfactant protein B gene responsible for fatal neonatal respiratory disease in multiple kindreds. *J. Clin. Invest.* 93:1860–1863.
12. Clark, J. C., S. E. Wert, C. J. Bachurski, M. T. Stahlman, B. R. Stripp, T. E. Weaver, and J. A. Whitsett. 1995. Targeted disruption of the surfactant protein B gene disrupts surfactant homeostasis, causing respiratory failure in newborn mice. *Proc. Natl. Acad. Sci. USA.* 92:7794–7798.
13. Melton, K. R., L. L. Nesslein, M. Ikegami, J. W. Tichelaar, J. C. Clark, J. A. Whitsett, and T. E. Weaver. 2003. SP-B deficiency causes respiratory failure in adult mice. *Am. J. Physiol.* 285:L543–L549.
14. Glasser, S. W., E. A. Detmer, M. Ikegami, C. L. Na, M. T. Stahlman, and J. A. Whitsett. 2003. Pneumonitis and emphysema in SP-C gene targeted mice. *J. Biol. Chem.* 278:14291–14298.
15. Baatz, J. E., B. Elledge, and J. A. Whitsett. 1990. Surfactant protein SP-B induces ordering at the surface of model membrane bilayers. *Biochemistry.* 29:6714–6720.
16. Vincent, J. S., S. D. Revak, C. G. Cochrane, and I. W. Levin. 1991. Raman spectroscopic studies of model human pulmonary surfactant systems: phospholipid interactions with peptide paradigms for the surfactant protein SP-B. *Biochemistry.* 30:8395–8401.
17. Schram, V., and S. B. Hall. 2004. SP-B and SP-C alter diffusion in bilayers of pulmonary surfactant. *Biophys. J.* 86:3734–3743.
18. Cochrane, C. G., and S. D. Revak. 1991. Pulmonary surfactant protein B (SP-B): structure-function relationships. *Science.* 254:566–568.
19. Longo, M. L., A. M. Bisagno, J. A. Zasadzinski, R. Bruni, and A. J. Waring. 1993. A function of lung surfactant protein SP-B. *Science.* 261: 453–456.
20. Lipp, M. M., K. Y. C. Lee, J. A. Zasadzinski, and A. J. Waring. 1996. Phase and morphology changes in lipid monolayers induced by SP-B protein and its amino-terminal peptide. *Science.* 273:1196–1199.
21. Lipp, M. M., K. Y. Lee, A. Waring, and J. A. Zasadzinski. 1997. Fluorescence, polarized fluorescence, and Brewster angle microscopy of palmitic acid and lung surfactant protein B monolayers. *Biophys. J.* 72:2783–2804.
22. Lee, K. Y. C., M. M. Lipp, J. A. Zasadzinski, and A. J. Waring. 1997. Effects of lung surfactant specific protein SP-B and model SP-B peptide on lipid monolayers at the air-water interface. *Colloid Surf. A Physicochem. Eng. Asp.* 128:225–242.
23. Takamoto, D. Y., M. M. Lipp, A. von Nahmen, K. Y. C. Lee, A. J. Waring, and J. A. Zasadzinski. 2001. Interaction of lung surfactant proteins with anionic phospholipids. *Biophys. J.* 81:153–169.
24. Pérez-Gil, J., J. Tucker, G. Simatos, and K. M. Keough. 1992. Interfacial adsorption of simple lipid mixtures combined with hydrophobic surfactant protein from pig lung. *Biochem. Cell Biol.* 70:332–338.
25. Yu, S. H., and F. Possmayer. 1990. Role of bovine pulmonary surfactant-associated proteins in the surface-active property of phospholipid mixtures. *Biochim. Biophys. Acta.* 1046:233–241.
26. Curstedt, T., H. Jornvall, B. Robertson, T. Bergman, and P. Berggren. 1987. Two hydrophobic low-molecular-mass protein fractions of pulmonary surfactant. Characterization and biophysical activity. *Eur. J. Biochem.* 168:255–262.
27. Whitsett, J. A., B. L. Ohning, G. Ross, J. Meuth, T. Weaver, B. A. Holm, D. L. Shapiro, and R. H. Notter. 1986. Hydrophobic surfactant-associated protein in whole lung surfactant and its importance for biophysical activity in lung surfactant extracts used for replacement therapy. *Pediatr. Res.* 20:460–467.

28. Hawgood, S., B. J. Benson, J. Schilling, D. Damm, J. A. Clements, and R. T. White. 1987. Nucleotide and amino acid sequences of pulmonary surfactant protein SP 18 and evidence for cooperation between SP 18 and SP 28–36 in surfactant lipid adsorption. *Proc. Natl. Acad. Sci. USA*. 84:66–70.

29. Wang, Z., S. B. Hall, and R. H. Notter. 1996. Roles of different hydrophobic constituents in the adsorption of pulmonary surfactant. *J. Lipid Res*. 37:790–798.

30. Oosterlaken-Dijksterhuis, M. A., H. P. Haagsman, L. M. G. van Golde, and R. A. Demel. 1991. Characterization of lipid insertion into monomolecular layers mediated by lung surfactant proteins SP-B and SP-C. *Biochemistry*. 30:10965–10971.

31. Notter, R. H., J. N. Finkelstein, and R. D. Taubold. 1983. Comparative adsorption of natural lung surfactant, extracted phospholipids, and artificial phospholipid mixtures to the air-water interface. *Chem. Phys. Lipids*. 33:67–80.

32. Hall, S. B., Z. Wang, and R. H. Notter. 1994. Separation of subfractions of the hydrophobic components of calf lung surfactant. *J. Lipid Res*. 35:1386–1394.

33. Discher, B. M., K. M. Maloney, D. W. Grainger, C. A. Sousa, and S. B. Hall. 1999. Neutral lipids induce critical behavior in interfacial monolayers of pulmonary surfactant. *Biochemistry*. 38:374–383.

34. Touchstone, J. C., J. C. Chen, and K. M. Beaver. 1980. Improved separation of phospholipids in thin layer chromatography. *Lipids*. 15:61–62.

35. Ames, B. N. 1966. Assay of inorganic phosphate, total phosphate and phosphatases. *Methods Enzymol*. VIII:115–118.

36. Searcy, R. L., and L. M. Bergquist. 1960. A new color reaction for the quantitation of serum cholesterol. *Clin. Chim. Acta*. 5:192–199.

37. Kaplan, R. S., and P. L. Pedersen. 1989. Sensitive protein assay in presence of high levels of lipid. *Methods Enzymol*. 172:393–399.

38. Schürch, S., H. Bachofen, J. Goerke, and F. Possmayer. 1989. A captive bubble method reproduces the in situ behavior of lung surfactant monolayers. *J. Appl. Physiol*. 67:2389–2396.

39. Putz, G., J. Goerke, S. Schürch, and J. A. Clements. 1994. Evaluation of pressure-driven captive bubble surfactometer. *J. Appl. Physiol*. 76: 1417–1424.

40. Crane, J. M., G. Putz, and S. B. Hall. 1999. Persistence of phase coexistence in disaturated phosphatidylcholine monolayers at high surface pressures. *Biophys. J*. 77:3134–3143.

41. Smith, E. C., J. M. Crane, T. G. Laderas, and S. B. Hall. 2003. Metastability of a supercompressed fluid monolayer. *Biophys. J*. 85:3048–3057.

42. Malcolm, J. D., and C. D. Elliott. 1980. Interfacial tension from height and diameter of a single profile drop or captive bubble. *Can. J. Chem. Eng*. 58:151–153.

43. Schoel, W. M., S. Schürch, and J. Goerke. 1994. The captive bubble method for the evaluation of pulmonary surfactant: surface tension, area, and volume calculations. *Biochim. Biophys. Acta*. 1200:281–290.

44. Goerke, J., and J. Gonzales. 1981. Temperature dependence of dipalmitoyl phosphatidylcholine monolayer stability. *J. Appl. Physiol*. 51:1108–1114.

45. Crane, J. M., and S. B. Hall. 2001. Rapid compression transforms interfacial monolayers of pulmonary surfactant. *Biophys. J*. 80:1863–1872.

46. Discher, B. M., W. R. Schief, V. Vogel, and S. B. Hall. 1999. Phase separation in monolayers of pulmonary surfactant phospholipids at the air-water interface: composition and structure. *Biophys. J*. 77:2051–2061.

47. Schief, W. R., M. Antia, B. M. Discher, S. B. Hall, and V. Vogel. 2003. Liquid-crystalline collapse of pulmonary surfactant monolayers. *Biophys. J*. 84:3792–3806.

48. Yan, W., S. C. Biswas, T. G. Laderas, and S. B. Hall. 2007. The melting of pulmonary surfactant monolayers. *J. Appl. Physiol*. 102: 1739–1745.

49. Yan, W., and S. B. Hall. 2006. Distribution of coexisting solid and fluid phases alters the kinetics of collapse from phospholipid monolayers. *J. Phys. Chem. B*. 110:22064–22070.

50. Rugonyi, S., E. C. Smith, and S. B. Hall. 2005. Kinetics for the collapse of trilayer liquid-crystalline disks from a monolayer at an air-water interface. *Langmuir*. 21:7303–7307.

51. Smith, E. C., T. G. Laderas, J. M. Crane, and S. B. Hall. 2004. Persistence of metastability after expansion of a supercompressed fluid monolayer. *Langmuir*. 20:4945–4953.

52. Rugonyi, S., E. C. Smith, and S. B. Hall. 2004. Transformation diagrams for the collapse of a phospholipid monolayer. *Langmuir*. 20: 10100–10106.

53. Tokieda, K., J. A. Whitsett, J. C. Clark, T. E. Weaver, K. Ikeda, K. B. McConnell, A. H. Jobe, M. Ikegami, and H. S. Iwamoto. 1997. Pulmonary dysfunction in neonatal SP-B-deficient mice. *Am. J. Physiol*. 273:L875–L882.

54. Nogee, L. M., D. E. de Mello, L. P. Dehner, and H. R. Colten. 1993. Brief report: deficiency of pulmonary surfactant protein B in congenital alveolar proteinosis. *N. Engl. J. Med*. 328:406–410.

55. Wang, Z., S. B. Hall, and R. H. Notter. 1995. Dynamic surface activity of films of lung surfactant phospholipids, hydrophobic proteins, and neutral lipids. *J. Lipid Res*. 36:1283–1293.

56. von Nahmen, A., A. Post, H. J. Galla, and M. Sieber. 1997. The phase behavior of lipid monolayers containing pulmonary surfactant protein C studied by fluorescence light microscopy. *Eur. Biophys. J. Biophys. Lett*. 26:359–369.

57. Ding, J., D. Y. Takamoto, A. von Nahmen, M. M. Lipp, K. Y. Lee, A. J. Waring, and J. A. Zasadzinski. 2001. Effects of lung surfactant proteins, SP-B and SP-C, and palmitic acid on monolayer stability. *Biophys. J*. 80:2262–2272.

58. Amrein, M., A. von Nahmen, and M. Sieber. 1997. A scanning force and fluorescence light microscopy study of the structure and function of a model pulmonary surfactant. *Eur. Biophys. J. Biophys. Lett*. 26: 349–357.

59. Krol, S., A. Janshoff, M. Ross, and H. J. Galla. 2000. Structure and function of surfactant protein B and C in lipid monolayers: a scanning force microscopy study. *Phys. Chem. Chem. Phys*. 2:4586–4593.

60. Lipp, M. M., K. Y. C. Lee, D. Y. Takamoto, J. A. Zasadzinski, and A. J. Waring. 1998. Coexistence of buckled and flat monolayers. *Phys. Rev. Lett*. 81:1650–1653.

61. Krol, S., M. Ross, M. Sieber, S. Kunneke, H. J. Galla, and A. Janshoff. 2000. Formation of three-dimensional protein-lipid aggregates in monolayer films induced by surfactant protein B. *Biophys. J*. 79: 904–918.

62. Otis, D. R., Jr., E. P. Ingenito, R. D. Kamm, and M. Johnson. 1994. Dynamic surface tension of surfactant TA: experiments and theory. *J. Appl. Physiol*. 77:2681–2688.

63. Bernardino de la Serna, J., J. Perez-Gil, A. C. Simonsen, and L. A. Bagatolli. 2004. Cholesterol rules: direct observation of the coexistence of two fluid phases in native pulmonary surfactant membranes at physiological temperatures. *J. Biol. Chem*. 279:40715–40722.

64. Hills, B. A. 1988. The Biology of Surfactant. Cambridge University Press, New York.

65. Schürch, S., H. Bachofen, J. Goerke, and F. Green. 1992. Surface properties of rat pulmonary surfactant studied with the captive bubble method: adsorption, hysteresis, stability. *Biochim. Biophys. Acta*. 1103: 127–136.

66. Follows, D., F. Tiberg, R. K. Thomas, and M. Larsson. 2007. Multilayers at the surface of solutions of exogenous lung surfactant: Direct observation by neutron reflection. *Biochim. Biophys. Acta*. 1768: 228–235.